Accepted Manuscript

Quinoxaline derivatives as new inhibitors of coxsackievirus B5

Antonio Carta, Giuseppina Sanna, Irene Briguglio, Silvia Madeddu, Gabriella Vitale, Sandra Piras, Paola Corona, Alessandra Tiziana Peana, Erik Laurini, Maurizio Fermeglia, Sabrina Pricl, Alessandra Serra, Elisa Carta, Roberta Loddo, Gabriele Giliberti

PII: S0223-5234(17)31114-5

DOI: 10.1016/j.ejmech.2017.12.083

Reference: EJMECH 10061

To appear in: *European Journal of Medicinal Chemistry*

Received Date: 26 June 2017

Revised Date: 19 December 2017

Accepted Date: 23 December 2017

Please cite this article as: A. Carta, G. Sanna, I. Briguglio, S. Madeddu, G. Vitale, S. Piras, P. Corona, A.T. Peana, E. Laurini, M. Fermeglia, S. Pricl, A. Serra, E. Carta, R. Loddo, G. Giliberti, Quinoxaline derivatives as new inhibitors of coxsackievirus B5, *European Journal of Medicinal Chemistry* (2018), doi: 10.1016/j.ejmech.2017.12.083.

QUINOXALINE DERIVATIVES AS NEW INHIBITORS OF COXSACKIEVIRUS B5

Antonio Carta, Giuseppina Sanna, Irene Briguglio, Silvia Madeddu, Gabriella Vitale, Sandra Piras, Paola Corona, Alessandra Tiziana Peana, Erik Laurini, Maurizio Fermeglia, Sabrina Pricl, Alessandra Serra, Elisa Carta, Roberta Loddo, Gabriele Giliberti

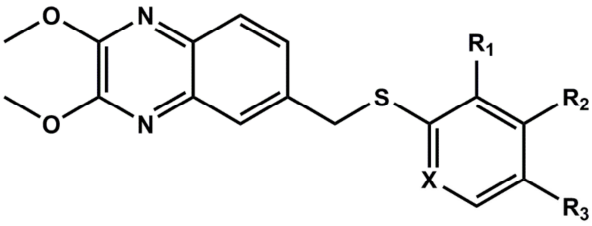

Potent activity against CV-B5

6) X = CH, R_1=H, R_2=H, R_3=COOEt
7) X = CH, R_1=H, R_2=H, R_3=COOH
8) X = N, R_1=H, R_2=H, R_3=COOEt

New quinoxaline derivatives emerged for their very potent antiviral activity against CV-B5.

Compound **6** inhibits the penetration, targeting the viral capsid protein VP1.

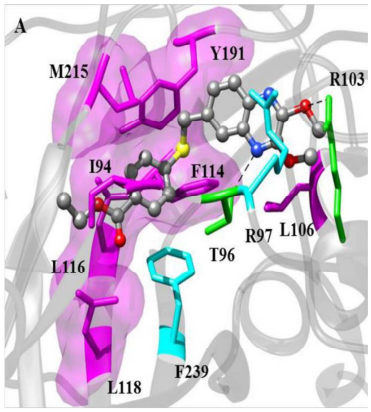

QUINOXALINE DERIVATIVES AS NEW INHIBITORS OF COXSACKIEVIRUS B5

Antonio Carta[a]**[1], Giuseppina Sanna[b]*[1], Irene Briguglio[a], Silvia Madeddu[b] , Gabriella Vitale[a], Sandra Piras[a], Paola Corona[a], Alessandra Tiziana Peana[a], Erik Laurini[c], Maurizio Fermeglia[c], Sabrina Pricl[c], Alessandra Serra[b], Elisa Carta[b], Roberta Loddo[b], Gabriele Giliberti[b]

[a] Department of Chemistry and Pharmacy, University of Sassari, Via Muroni 23, 07100 Sassari, Italy.

[b] Department of Biomedical Sciences, University of Cagliari, Cittadella Universitaria, 09042 Monserrato, Cagliari, Italy.

[c] Molecular Simulation Engineering (MOSE) Laboratory, University of Trieste, Piazzale Europa 1, 34127 Trieste, Italy.

[1] Equal contribution

* Corresponding author: Dr. Giuseppina Sanna.

E-mail: g.sanna@unica.it. Phone: +39-070-6754161.

** Co-Corresponding author: Antonio Carta.

E-mail: acarta@uniss.it. Phone: +39-079-228722.

Abstract

Enteroviruses are among the most common and important human pathogens for which there are no specific antiviral agents approved by the US Food and Drug Administration so far. Particularly, coxsackievirus infections have a worldwide distribution and can cause many important diseases. We here report the synthesis of new 14 quinoxaline derivatives and the evaluation of their cytotoxicity and antiviral activity against representatives of ssRNA, dsRNA and dsDNA viruses. Promisingly, three compounds showed a very potent and selective antiviral activity against coxsackievirus B5, with EC_{50} in the sub-micromolar range (0.3 - 0.06 µM). A combination of experimental techniques (i.e. virucidal activity, time of drug addition and adsorption assays) and *in silico* modeling studies were further performed, aiming to understand the mode of action of the most active, selective and not cytotoxic compound, the ethyl 4-[(2,3-dimethoxyquinoxalin-6-yl)methylthio]benzoate (**6**).

Keywords: antiviral activity; enteroviruses; viral protein VP1; in silico modeling.

1. Introduction

Viral infections are the major cause of morbidity and mortality in elderly people and young children worldwide, since in many of these instances no antiviral agents are available in the clinic. Enteroviruses (EVs), for instance, are pathogens circulating commonly in the environment, with a seasonal peak during early fall. They belong to the *Picornaviridae* family, characterized by a single-stranded positive RNA genome surrounded by an icosahedral capsid around 30 nm in size [1]. Enteroviruses, which include coxsackievirus A and B, poliovirus and echoviruses, cause systemic infection in man after ingestion and replication in the gastrointestinal tract [2]. The infection is normally asymptomatic or mild, but occasionally the virus spreads to secondary organs leading to more severe diseases such as aseptic meningitis or myocarditis [3, 4]. EVs have long been associated with various diseases of man resulting into a wide range of acute symptoms involving

the cardiac and skeletal muscles, the central nervous system, the pancreas, the skin and mucous membranes [5, 6]. Their roles in chronic diseases have also been proposed [7, 8]. Particularly, coxsackieviruses are non-enveloped viruses classified into two distinct groups A and B. Group A coxsackieviruses (CV-A) were noted to cause a flaccid paralysis, due to generalized myositis, while group B coxsackieviruses (CV-B) were linked to spastic paralysis due to focal muscle injury and degeneration of neuronal tissue. The last group are also prone to infect the heart, pleura, pancreas, and liver, causing pleurodynia, myocarditis, pericarditis, and hepatitis [9]. In particular, coxsackie B viruses are an important cause of myopericarditis in children and adults and are associated with the pathogenesis of the dilated cardiomyopathy [10, 11]. Also a systemic neonatal disease is often associated with the group B coxsackieviruses [12]. Indeed, coxsackievirus B has also been detected in the amniotic fluid, placenta, and tissue of unborn children indicating the ability of pregnant women to transmit the virus [13].

Coxsackievirus B5 (CV-B5) is one of the six serotypes of CV-B; it is associated with encephalitis and myocarditis in immunocompromised children and central nervous system disease in the elderly adults [14].

Notwithstanding the incredible efforts and progresses in the antiviral field, conventional drug therapies targeted against most of ssRNA, dsRNA and dsDNA viral infections remains limited, often with poor efficacy and incomplete coverage. Because of these limitations, basic antiviral drug discovery programs still constitute the fundamental cornerstone in the development of new and more effective antiviral arsenals.

In this scenario, the present study investigates the antiviral activities of newly synthesized quinoxaline derivatives on a panel of selected viruses. Nowadays nitrogen containing heterocyclic compounds represent one of the largest areas of research in organic chemistry and have been extensively studied for their broad range of biological activity [15]. Particularly, the quinoxaline scaffold is described as a bioisoster of quinoline, naphthalene and benzothiophene [16]; specifically, suitably functionalized polysubstituted quinoline and quinoxaline derivatives can boast different

biological properties [17], including antibacterial [18], antitubercular [19-21], antifungal [22, 23], antitumoral [24, 25], antinflammatory [26], P-glycoprotein-mediated drug efflux inhibitor [27] and antiviral activities [17]. Actually various quinoxaline derivatives (Figure 1) were investigated for their activity against viruses such as HSV-1 (compound **A**) [28], influenza (compound **B**) [29], HIV-1 (compound **C** and compound **D**) [30, 31]. Notably, compound **D**, equally functionalized on positions 6 and 7 and bearing an aliphatic chain in position 2, is endowed with selective anti-HIV-1 activity, showing an $EC_{50} = 0.22 \pm 0.08$ µg/ml.

In this paper we present a series of 14 new quinoxaline derivatives (**2a-e, 3-11)** which structures are reported in Figure 2.

All compounds were tested against a selected panel of ssRNA, dsRNA and dsDNA viruses, which includes several important human pathogens such as Human immunodeficiency virus (HIV-1) and Respiratory syncytial virus (RSV), for which the efficacy of therapeutic agents is unsatisfactory. Quite importantly, among the whole set of the new quinoxaline derivatives one particular compound, derivative **6**, showed a remarkable activity against CV-B5 virus ($EC_{50} = 0.09$ µM) and selectivity, with absence of cytotoxicity ($CC_{50} > 100$ µM) towards the Vero-76 cells. Accordingly, this compound was selected for further experimental/*in silico* investigations aimed at determining its mechanism of action. In particular, time-of-drug-addition studies revealed that compound **6** might interfere with the earliest stages of viral replication while computer-assisted molecular simulations highlighted the existence of multiple hydrophobic, polar and hydrogen bond interactions between the compound and the external viral capsid protein (VP1).

2. Results and discussion

2.1. Chemistry

Quinoxaline derivatives **2a-e, 3-5** were prepared according to the chemical pathways reported in Scheme 1, while compounds **6-11** were prepared according to Scheme 2.

Briefly, the key intermediate 6-(bromomethyl)-2,3-dimethoxyquinoxaline was obtained following the procedures described by Loriga et al. [32]. Its reaction with the appropriate benzenethiol derivative derivatives (**1a-d**) was carried out in DMF at 70 °C to give the expected compounds **2a-d**. Condensation between the same intermediate and the pyridine-2-thiol (**1e**) in DMF, in presence of Cs_2CO_3, gave the expected derivative **2e**. From compound **2d** *via* basic hydrolysis the corresponding carboxylic acid **3** was obtained. This compound was amidified with L-glutamic acid diethyl ester hydrochloride in DMF in presence of triethylamine (TEA) and diethyl dicarbonate (DEPC) to give derivative **4**. The free acid **5** was finally obtained from compound **4** by alkaline hydrolysis.

Compounds **6** and **8** were obtained by an alternative pathway using a solution of diethyl 4,4'-dithiodibenzoate (**12a**) or diethyl 6,6'-dithionicotinate (**12b**) treated with $NaBH_4$ under nitrogen. The unisolated sodium thiolate derivatives, in presence of 6-(bromomethyl)-2,3-dimethoxyquinoxaline, react in DMF to give, respectively, the benzoate derivative **6** and the nicotinate derivative **8** with good yields. Ester hydrolysis under basic conditions gave the corresponding acid derivatives **7** and **9**. Amide derivative **10** was subsequently obtained for reaction of the corresponding free acid **9** with diethyl L-glutamate. Finally, alkaline hydrolysis of amide compound **10** gave the corresponding L-glutamic acid derivative **11**.

2.2. Biology

All synthesized quinoxalines derivatives were tested in cell-based assays against representative of several RNA and DNA virus families. The results are reported in the Table 1. Compounds that haven't showed any antiviral activity or cytotoxicity are not present in the table.

Table 1. Antiviral activity of quinoxaline derivatives against RNA and DNA viruses and cytotoxicity against the cell lines used in the assays.

Compounds	MT-4	HIV-1	MDBK cells	BVDV	BHK cells	YFV, Reo-1	Vero-76 cells	CV-B5	Sb-1, RSV, VSV, VV, HSV-1
	CC_{50}[a]	EC_{50}[b]	CC_5[c]	EC_{50}[d]	CC_{50}[e]	EC_{50}[f]	CC_{50}[g]	EC_{50}[h]	EC_{50}[i]
2b	48	>48	>100	>100	80	>80	75	>75	>75
2c	>100	**36 S.I. >2.7**	>100	>100	>100	>100	>100	>100	>100
2e	28	>28	>100	>100	>100	>100	>100	>100	>100
4	60	>60	>100	>100	>100	>100	>100	>100	>100
6	>100	>100	>100	>100	>100	>100	>100	**0.09 ± 0.01 S.I. >1111**	>100
7	68	>68	>100	>100	65	>65	65	**0.06 ± 0.01 S.I.= 1083**	>65
8	>100	>100	>100	>100	>100	>100	>100	**0.3 ± 0.05 S.I. >333**	>100
9	>100	>100	>100	>100	>100	>100	90	**3.8 ± 0.5 S.I.= 23**	>90
10	19	>19	>100	**10 ± 1.4 S.I. >10**	85	>85	>100	**56 S.I. >1.7**	>100
References									
Efavirenz	40	0.002 ± 0.0002							
2'-C-methyl-guanosine			>100	1.1 ± 0.1	>100	1.9 ± 0.1			
Pleconaril							>100	0.005 ± 0.001	

Data represent mean values for three independent determinations. Standard deviations are reported for the more active compounds. Also for the others values the variation was less than 15%.

[a]Compound concentration (μM) required to reduce the proliferation of mock-infected MT-4 cells by 50%. [b]Compound concentration (μM) required to achieve 50% protection of MT-4 cells from HIV-1 induced cytopathogenicity. [d,f]Compound concentration (μM) required to achieve 50% protection of MDBK and BHK cells from BVDV-induced[(d)] and YFV or Reo-1-induced cytopathogenicity[(f)]. [c,e,g]Compound concentration (μM) required to reduce the viability of mock-infected MDBK[(c)], BHK[(e)] and Vero-76[(g)] cells by 50%. [h,i]Compound concentration (μM) required to reduce the plaque number of CV-B5[(h)] and Sb-1, RSV, VSV, VV, HSV-1[(i)] by 50% in Vero-76 monolayers.

S.I. = Selectivity index (CC_{50}/EC_{50})

As seen from Table 1, compound **10** showed a moderate activity against BVDV (10 μM) and CV-B5 (56 μM). A selective anti-HIV-1 activity, although not very potent (EC_{50} = 36 μM), was found for **2c**. On the other hand, four compounds (**6**, **7**, **8**, **9**) emerged for their very potent antiviral

activity (EC_{50} = 0.06 - 3.8 µM) against CV-B5. For compounds bearing a functionalized phenyl moiety, best results were obtained when a carboxylic group is located on position 4: the benzoate derivative **6** and its acidic derivative **7** emerged for their potency (0.09 and 0.06 µM, respectively) and selectivity. For the nicotinate series, again a carboxylic group on the aromatic side ring in para position to the thiomethyl chain led to the best results. However, in this case, the ester **8** was found almost 13 times more potent than the corresponding acid **9** (0.3 and 3.8 µM, respectively). Since compound **6** showed the most potent and highest selective activity against CV-B5 (EC_{50} = 0.09 ± 0.01 µM), and no cytotoxicity against mammalian cells [selectivity index (S.I.) >1000], it was selected for further characterization.

Accordingly, the antiviral activity of **6** was investigated in a yield reduction assay, in order to ascertain the reduction of virus titre in the presence of the active compound during a single round of viral infection. Not cytotoxic concentrations of 20, 4, 0.8 and 0.16 µM were used and a dose-dependent reduction of virus titre was observed, with a significant reduction of titre already at very low concentrations (Figure 3).

The potential virucidal activity of **6** was also investigated, incubating a CV-B5 solution containing 5×10^5 PFU/ml for 1 hour at 37 °C with two concentrations of compound (4 and 20µM). Compound **6** failed to affect the CV-B5 infectivity (data not showed), suggesting that the inhibition of CV-B5 replication observed in cell-based assays is not due to the infectivity inactivation of virions, but can be ascribed to an interference of compounds with the viral life cycle.

Experiments designed to test the mechanism of action of **6** under a single cycle conditions on intracellular virus replication showed (Figure 4) prominent inhibitory activity in decreasing plaque formation between 0 and 2 hours post infection.

Pretreatment with **6** or addition of **6** simultaneously to infection, followed by the removal of the sample after two hours, did not result in virus titre reduction (data not showed). On the contrary, the addition of **6** simultaneously or at 2 hours post infection significantly reduces the virus titre, while the compound addition at 4, 6, 8 or 12 hours post-infection completely failed to reduce the virus

titre, in analogy with the untreated control. These data suggest that **6** inhibits CV-B5 infection by targeting the early events of attachment, entry or uncoating.

To better define the process of inhibition, the kinetics of virus adsorption in the presence of **6** was next evaluated. As a matter of fact, low-temperature treatment allows binding of viruses to the cell surface receptors but prevents the internalization of virus particles into the cells [33, 34]. Accordingly, Vero-76 cells were incubated with CV-B5 (m.o.i. = 0.1) and **6** for different times at 4 °C, using compound concentrations of 20 and 4μM, respectively. The treatment with compound **6** did not result in detectable reduction of the virus titre in comparison to untreated infected control, suggesting that inhibition occurs after the adsorption step.

2.3. Modeling results

Given all these experimental evidences and the further observation that the activity of **6** towards CV-B5 is approximately 10 time less higher (EC_{50} = 0.09 μM) that the one measured for the same cell line treated with pleconaril (EC_{50} = 0.005 μM, Table 1), the hypothesis that these two compounds might exert a similar mechanism of action as viral capsid protein binders was formulated. Indeed, similarly to more intensively studied and characterized Rhinovirus, the CV-B virion structure exhibits an icosahedral symmetry with a diameter size of approximately 30 nm [35]. Four capsid proteins (VP1-VP4) comprise the virion structure, VP1-VP3 being three external capsid proteins while protein VP4 is located on the inside of the capsid shell. Accordingly, a large cleft (aka as canyon) on each of the icosahedral faces of the capsid is the site for interaction with the host cell receptor [36]. Below this canyon, a hydrophobic pocket is present that in nature, at least for Rhinovrus, is occupied by a 'pocket factor', proposed to be a lipid or fatty acid [37]. This pocket has been implicated in the conformational changes that VP1 needs to undergo during infection of the host cell [38]. A panel of rhinovirus inhibitors, referred to as capsid binders (e.g. pleconaril (Schering-Plough) and vapendavir (Biota Pharmaceuticals)), are known to insert into this hydrophobic pocket, and to stabilize the capsid, thus blocking virus-receptor binding and uncoating.

Under this perspective, the validity of postulated molecular mechanism of action of **6** was checked via computer-assisted molecular simulations. Figure 5 offers a global view of the molecular dynamics (MD) optimized VP1-VP4 capsid protein system in complex with **6**.

The relevant MM/PBSA analysis yielded a good binding affinity of the molecule for the protein (ΔG_{bind} = -9.80 ± 0.31 kcal/mol, corrsponding to a calculated value of $EC_{50,calc}$ = 0.13 μM), in agreement with its inhibition activity (Table 1). The main favorable contribution to ΔG_{bind} is provided by the van der Waals (-37.12 ± 0.08 kcal/mol) and electrostatic (-19.57 ± 0.14 kcal/mol) components in the gas phase, while the solvation (+20.33 ± 0.12 kcal/mol) and entropic (+26.56 ± 0.24 kcal/mol) components oppose binding.

The specific VP1/**6** binding mode (Figure 6(A)) was analyzed by a per-residue decomposition of the enthalpic component of the free energy of binding $\Delta H_{bind,res}$. These data (Figure 6(B)) revealed that in the VP1/**6** complex the compound hydrocarbon scaffold established mostly hydrophobic interactions with VP1 residues I94, L106, F114, L116, L118, Y191, and M215.

Compound **6** is further permanently hydrogen-bonded to the hydroxyl group of T96 via one of the quinoxaline nitrogen atom (average dynamic length (ADL) = 3.12 ± 0.04 Å) and to donor guanidinic group of R103 by its acceptor methoxyl oxygen (ADL = 2.99 3.12 ± 0.05 Å). This analysis further identified a π-π interaction through a t-shape conformation between the substituted phenyl ring of **6** and the aromatic side chain of F239, and a π-cation bond involving the quinoxaline aromatic ring and the positive charged R97. As it can be seen from Figure 6(B), all the involved residues provided a substantial contribution in stabilizing the intermolecular complex enthalpy since all $\Delta H_{bind,res}$ values higher than |0.75 kcal/mol|, suggesting a quite strong interaction of the VP1 viral protein with compound **6**.

3. Conclusions

In this work we reported the synthesis of new quinoxaline derivatives and the determination of their antiviral activity against a panel of representative ssRNA$^+$, ssRNA$^-$, dsRNA and DNA viral families, cytotoxicity against different cell lines (MT-4, MDBK, BHK and Vero-76). Among all compounds, three molecules resulted endowed negligible cytotoxicity and strong and highly selective activity against the coxsackievirus CV-B5, with EC_{50} values in the range 0.3 – 0.06 μM. In this small set, compound **6**, (EC_{50} = 0.09 μM and SI >100) was selected for further experimental/computational investigations aimed at assessing its possible molecular-based mechanism of viral replication inhibition.

To the purpose, a series of experiments including virucidal activity, time of addition and virus adsorption assays were first carried out. The results of these experiments suggested that **6** did not interfere with the viral attachment to cell receptors, but, rather, it prevented infection by targeting the subsequent penetration step or an early event during the life cycle. Molecular simulations revealed that a possible viral target for compound **6** is the viral capsid protein VP1. In analogy with other molecules such as pleconaril (which exhibits only a 10-times higher EC_{50} value with respect to **6**), the potent quinoxaline derivative **6** can favourably insert into a hydrophobic pocket of the VP1 chain of the capsid protomer implicated in the protein conformational changes during infection of the host cell. Accordingly, by locking the pocket into a ligand-bond conformation may prevents the internalization of virus particles.

Coxsackieviruses B are members of Enterovirus genus (*Picornaviridae* family) and represent important human pathogens that cause both acute and chronic diseases in infants, young children and immunocompromised individuals. Until now, there is no enterovirus-specific vaccine or therapeutic reagent available for clinical use. Our studies show that the present new quinoxaline derivatives, possessing high activity and selectivity accompanied with very low cytotoxicity may serve as a good starting point for the development of novel drugs for the treatment of infections by Enterovirus.

4. Experimental

4.1. Chemistry

Melting points were carried out with a Köfler hot stage or Digital Electrothermal melting point apparatus. Infrared spectra were recorded as nujol mulls with a Perkin-Elmer 781. Nuclear magnetic resonance (^{1}H-NMR and ^{13}C-NMR) spectra were determined in $CDCl_3$ or DMSO-d_6 and were recorded with a Bruker Avance III 400 NanoBay. Chemical shifts are reported in parts per million (ppm) downfield from tetramethylsilane (TMS) used as internal standard. Splitting patterns are designated as follows: s, singlet; d, doublet; t, triplet; q, quadruplet; m, multiplet; br s, broad singlet; dd, double doublet.

Mass spectra (MS) were performed on combined Liquid Chromatograph-Agilent 1100 series Mass Selective Detector (MSD). Analytical thin-layer chromatography (TLC) was performed on Merck silica gel F-254 plates. Pure compounds showed a single spot in TLC. For flash chromatography, Merck silica gel 60 was used with a particle size 0.040-0.063 mm (230-400 mesh ASTM). Elemental analysis were performed on a Perkin-Elmer 2400 instrument and the results were within ± 0.4% of theoretical values.

4.1.2. Starting material and known intermediates

Key intermediates 6-(bromomethyl)-2,3-dimethoxyquinoxaline, diethyl 4,4'-dithiodibenzoate (**12a**) and diethyl 6,6'-dithiodinicotinate (**12b**) were prepared according to the procedures described in the literature [32, 39]. Benzenethiol derivatives (**1a-d**) and the pyridine-2-thiol (**1e**) were commercially available. Details of synthesis of each compound are following provided.

4.1.3. General procedure for the preparation of 6-[(het)arylthiomethyl]quinoxalines derivatives 2a-e.

Equimolar amounts (2 mmol) of 6-(bromomethyl)-2,3-dimethoxyquinoxaline and the suitably benzenethiol derivative (**1a-d**) or pyridine-2-thiol (**1e**) were stirred in dry DMF (8 ml) with an excess of Cs_2CO_3 at 70 °C for 2.5 h. After cooling and dilution with water, compounds **2a-e**

precipitated as solids, which were collected by filtration and washed with water. All compounds, obtained as light colored powders, were purified by recrystallization from EtOH/H_2O.

4.1.3.1. *2,3-dimethoxy-6-[(4-methoxyphenyl)thiomethyl]quinoxaline (**2a**).* Yield 83%. M.p. 90-91 °C. ν_{max} cm^{-1}: 1600; 1220; 1090; 1035. λ_{max} nm: 331; 316; 248; 214; 203. ^{1}H-NMR (DMSO-d_6) δ: 7.67 (1H, d, $J_{8,7}$=8.4 Hz, H-8), 7.65 (1H, s, H-5), 7.36 (1H, d, J=8.4 Hz, H-7), 7.26 (2H, d, J=8.6 Hz, H-3',5'), 6.77 (2H, d, J=8.6 Hz, H-2',6'), 4.14 (3H, s, OCH_3), 4.49 (2H, s., CH_2), 4.12 (3H, s, OCH_3), 3.77 (3H, s, 4'-OCH_3). ^{13}C-NMR (DMSO-d_6) δ: 157.03 (C), 149.12 (C), 148.98 (C), 136.23 (C), 135.54 (C), 135.36 (C), 130.42 (2 CH), 127.50 (CH), 127.02 (C), 126.21 (CH), 125.95 (CH), 114.53 (2 CH), 54.79 (CH_3), 53.75 (2 CH_3), 34.89 (CH_2). LC/MS: 343 (M + H). Anal. Calcd for $C_{18}H_{18}N_2O_3S$ C, 63.14; H, 5.30; N, 8.18; S, 9.36. Found C, 63.20; H, 5.28; N, 8.12; S, 9.42.

4.1.3.2. *6-[(3,4-dichlorophenyl)thiomethyl]-2,3-dimethoxyquinoxaline (**2b**).* Yield 89%. M.p. 76-77 °C. ν_{max} cm^{-1}: 1600; 1225; 1130; 1090; 1035; 800. λ_{max} nm: 330; 316; 249; 211. ^{1}H-NMR (DMSO-d_6) δ: 7.70 (1H, d, J=8.4 Hz, H-8), 7.65 (1H, s, H-5), 7.45 (1H, d, J=1.8 Hz, H-2'), 7.39 (1H, d, J=8.4 Hz, H-7), 7.28 (1H, d, J=8.2 Hz, H-5'), 7.09 (1H, d, J=8.2 Hz, H-6'), 4.46 (2H, s, CH_2), 4.00 (6H, s, 2,3-OCH_3). ^{13}C-NMR (DMSO-d_6) δ: 155.14 (C), 154.98 (C), 137.25 (C), 136.30 (C), 135.65 (C), 135.50 (C), 131.42 (C), 130.55 (CH), 129.18 (CH), 128.25 (C), 128.11 (CH), 127.53 (CH), 126.11 (CH), 125.90 (CH), 53.87 (2 CH_3), 35.92 (CH_2). LC/MS: 381 (M + H). Anal. Calcd for $C_{17}H_{14}Cl_2N_2O_2S$: C, 53.55; H, 3.70; Cl, 18.60; N, 7.35; S, 8.41. Found C, 53.60; H, 3.67; Cl, 18.70; N, 7.34; S, 8.37.

4.1.3.3. *2,3-dimethoxy-6-[(naphthalen-2-yl)thiomethyl]quinoxaline (**2c**).* Yield 24%. M.p. 91-92 °C. ν_{max} cm^{-1}: 1600; 1530. λ_{max} nm: 330; 316; 249; 216. ^{1}H-NMR ($CDCl_3$) δ: 7.77-7.70 (6H, m, arom), 7.51-7.45 (4H, m, arom), 4.37 (2H, s, CH_2), 4.15 (3H, s, CH_3O), 4.13 (3H, s, CH_3O). ^{13}C-NMR ($CDCl_3$) δ: 150.12 (C), 149.96 (C), 137.10 (C), 136.39 (C), 136.09 (C), 133.71 (C), 133.67 (C), 131.94 (C), 128.40 (CH), 127.90 (CH), 127.76 (CH), 127.69 (CH), 127.59 (CH),127.18 (CH), 126.55 (CH), 126.48 (CH), 126.31 (CH), 125.79 (CH), 54.24 (2 CH_3), 38.90 (CH_2). LC/MS: 362

279 (M + H). Anal. Calcd for $C_{21}H_{19}N_2O_2S$: C, 69.59; H, 5.01; N, 7.73; S, 8.85. Found C, 69.65; H,
280 5.11; N, 7.64; O, 8.76; S, 8.88

281 **4.1.3.4.** *Methyl 2-[(2,3 dimethoxyquinoxalin-6-yl)methylthio]benzoate (**2d**).* Yield 85%. M.p. 142-
282 143 °C. ν_{max} cm^{-1}: 1720; 1580; 1220; 1115; 1070; 1000. λ_{max} nm: 330; 315; 248; 213. ^{1}H-NMR
283 (DMSO-d_6) δ: 7.89 (1H, d, J=7.2 Hz, H-6'), 7.80 (1H, s, H-5), 7.69 (1H, d, J=8.0 Hz, H-7), 7.59-
284 7.502 (2H, m, H-8 + H-5'), 7.22 (1H, m, H-4'), 4.40 (2H, s, CH_2), 4.01 (6H, s, 2 OCH_3), 3.81 (3H,
285 s, OCH_3). ^{13}C-NMR (DMSO-d_6) δ: 166.05 (C), 149.94 (C), 149.76 (C), 140.53 (C), 136.37 (C),
286 135.64 (C), 135.35 (C), 132.64 (CH), 130.70 (CH), 127.79 (CH), 127.05 (C), 126.25 (CH), 126.09
287 (CH), 126.05 (CH), 124.32 (CH), 53.89 (2 CH_3), 52.06 (CH_3), 35.30 (CH_2). LC/MS: 371 (M + H).
288 Anal. Calcd for $C_{19}H_{18}N_2O_4S$: C, 61.61; H, 4.90; N, 7.56; S, 8.65. Found C, 61.70; H, 4.83; N, 7.58;
289 S, 8.57

290 **4.1.3.5.** *2,3-dimethoxy-6-[(pyridin-2-yl)thiomethyl]quinoxaline (**2e**).* Yield 90%. M.p. 118-119 °C.
291 ν_{max} cm^{-1}: 1580. λ_{max} nm: 330; 315; 302; 212; 196. ^{1}H-NMR (DMSO-d_6) δ: 8.48 (1H, d, J=4.4 Hz,
292 H-6'), 7.76 (1H, s, H-5), 7.68-7.63 (2H, m, H-8 + H-4'), 7.56 (1H, d, J=7.2 Hz, H-7), 7.33 (1H, d, J
293 = 8.4 Hz, H-3'), 7.13 (1H, m, H-5'), 4.59 (2H, s, CH_2), 4.01 (6H, s, 2 OCH_3). ^{13}C-NMR (DMSO-d_6)
294 δ: 157.72 (C), 149.93 (C), 149.70 (C), 149.39 (C), 136.96 (C), 136.74 (CH), 136.31 (C), 135.53 (C),
295 127.69 (CH), 126.02 (CH), 125.73 (CH), 121.69 (CH), 120.03 (CH), 53.88 (2 CH_3), 32.80 (CH_2).
296 LC/MS: 314 (M + H). Anal. Calcd for $C_{16}H_{15}N_3O_2S$: C, 61.32; H, 4.82; N, 13.41; S, 10.23. Found
297 C, 61.26; H, 4.78; N, 13.35; S, 10.27.

298 **4.1.4. General procedure for the preparation of ethyl 4-[(2,3-dimethoxyquinoxalin-6-**
299 **yl)methylthio]benzoate (6) and ethyl 6-[(2,3-dimethoxyquinoxalin-6-yl)methylthio]nicotinate**
300 **(8)**

301 $NaBH_4$ (2.5 mmol) was added to a solution of diethyl 4,4'-dithiodibenzoate (**12a**) or diethyl 6,6'-
302 dithionicotinate (**12b**) (2.50 mmol) in 25 ml of absolute ethanol under N_2. The corresponding
303 solution was stirred for 30′. This solution was slowly (15′) added to a solution of 6-(bromomethyl)-

2,3-dimethoxyquinoxaline (3.00 mmol) in 10 ml of DMF. The mixture was stirred, at room temperature, for 5 h. After dilution with water the precipitated products were collected and washed with water. Compounds **6** and **8** were obtained as white powder and were further purified by crystallization from EtOH/H_2O.

4.1.4.1. *Ethyl 4-[(2,3-dimethoxyquinoxalin-6-yl)methylthio]benzoate (**6**).* Yield 64%. M.p. 130-131 °C ν_{max} cm^{-1}: 1705; 1225; 1175; 1090. λ_{max} nm: 329; 315; 301; 295; 247; 211. ^{1}H-NMR (DMSO-d_6) δ: 7.83 (2H, d, J = 8.8 Hz, H-2' + H-6'), 7.73 (1H, s, H-5), 7.70 (1H, d, J=8.4 Hz, H-8), 7.59 (1H, d, J = 8.4 Hz, H-7), 7.48 (2H, d, J = 8.8 Hz, H-3' + H-5'), 4.53 (2H, s, CH_2S), 4.27 (2H, q, OCH_2CH_3), 4.02 (6H, m, 2 CH_3), 1.28 (3H, t, CH_3). ^{13}C-NMR (DMSO-d_6) δ: 165.89 (C), 150.02 (C), 149.83 (C), 143.25 (C), 136.33 (C), 135.66 (C), 135.61 (C), 129.48 (2 CH), 127.61 (CH), 126.59 (CH), 126.52 (C), 126.15 (CH), 125.89 (2 CH), 60.60 (CH_2), 53.92 (2 CH_3), 34.86 (CH_2), 14.11 (CH_3).

4.1.4.2. *Ethyl 6-[(2,3-dimethoxyquinoxalin-6-yl)methylthio]nicotinate **(8).*** Yield 95%. M.p. 105-106 °C. ν_{max} cm^{-1}: 1720; 1585. λ_{max} nm: 329; 315; 302; 248; 211. ^{1}H-NMR (DMSO-d_6) δ: 8.94 (1H, s, H-6'), 8.06 (1H, d, J=8 Hz, H-4'), 7.77 (1H, s, H-5), 7.67 (1H, d, J=8.4 Hz, H-7), 7.59 (1H, d, J=8 Hz, H-3'), 7.47 (1H, d, J=8.4 Hz, H-8) 4.65 (2H, s, CH_2S), 4.31 (2H, q, CH_2CH_3), 4.01 (6H, s, 2 CH_3O), 1.31 (3H, t, CH_3CH_2). ^{13}C-NMR (DMSO-d_6) δ: 167.64 (CO), 164.53 (C), 163.73 (C), 149.93 (CH), 149.76 (C),136.69 (CH), 136.30 (2 C), 135.63 (C), 127.71 (CH), 126.11 (CH), 125.88 (CH), 121.92 (C), 121.23 (CH), 60.94 (CH_2), 53.89 (2 CH_3), 32.97 (CH_2), 14.04 (CH_3). LC/MS: 386 (M + H). Anal. Calcd for $C_{19}H_{19}N_3O_4S$: C, 59.21; H, 4.97; N, 10.90; S, 8.32. Found C, 59.17; H, 5.03; N, 10.85; S, 8.44.

4.1.5. General procedure for the preparation of 2 and 6-[(2,3-dimethoxyquinoxalin-6-yl)methylthio]benzoic acids (3,7), and 6-[(2,3-dimethoxyquinoxalin-6-yl)methylthio]nicotinic acid (9).

A mixture of 2 mmol of the suitable ester (**2d**,**6,8**) in 30 ml of hydroalcoholic solution 1:2 and 10 ml of 1N NaOH was stirred at 70° C, for 7 h. After cooling, the ethanol was evaporated in vacuo and the alkaline aqueous solution was diluted with water and made acidic using HCl 2M. The product obtained by precipitation was collected and washed with water. Acid derivatives **3** and **9** were purified by crystallization from EtOH/H_2O, while derivative **7** by flash cromatography (eluant: mixture $CHCl_3$-MeOH 95:5).

4.1.5.1. *2[(2,3-dimethoxyquinoxalin-6-yl)methylthio]benzoic acid (**3**).* Yield 82%. M.p. 241-242 °C. ν_{max} cm^{-1}: 1690; 1590; 1225; 1090; 1060; 995. λ_{max} nm: 330; 316; 249; 215. ^{1}H-NMR (DMSO-d_6) δ: 7.88 (1H, d, J=7.6 Hz, H-6'), 7.81 (1H, s, H-5), 7.67 (1H, d, J=8.4 Hz, H-7), 7.57 (1H, d, J=7.2 Hz, H-4'), 7.50-7.47 (1H, m, H-3'), 7.20-7.10 (1H, m, H-5'), 4.45 (2H, s, CH_2S), 4.00 (6H, s, 2 CH_3O. ^{13}C-NMR (DMSO-d_6) δ: 167.88 (CO), 150.36 (C), 150.17 (C), 141.34 (C), 136.88 (C),136.08 (C), 135.91 (C), 132.77 (CH), 131.40 (CH), 128.30 (CH), 128.20 (C), 126.52 (2 CH), 126.21 (CH), 124.48 (CH), 54.34 (2 CH_3), 35.75 (CH_2). LC/MS: 357 (M + H). Anal. Calcd for $C_{19}H_{16}N_2O_4S$: C, 60.66; H, 4.53; N, 7.86; S, 9.00. Found C, 60.59; H, 4.55; N, 7.80; S, 9.08.

4.1.5.2. *4-[(2,3-dimethoxyquinoxalin-6-yl)methylthio]benzoic acid (**7**).* Yield 47%. M.p. 195-196 °C. ν_{max} cm^{-1}: 1710; 1590; 1215; 1090; 990. λ_{max} nm: 330; 316; 290; 248; 212. ^{1}H-NMR (DMSO-d_6) δ: 7.82 (2H, d, J=8.4 Hz, H-3' + H-5'), 7.72 (1H, s, H-5), 7.65 (1H, d, J=8.4 Hz, H-8), 7.54 (1H, d, J=8.4 Hz, H-7), 7.42 (2H, d, J=8.4 Hz, H-2' + H-6'), 4.44 (2H, s, CH_2), 3.99 (6H, s, 2 CH_3). ^{13}C-NMR (DMSO-d_6) δ: 166.87 (C), 149.91 (C), 149.72 (C), 142.70 (C), 136.35 (C), 135.63 (C), 135.45 (C), 129.69 (2 CH), 127.46 (CH), 127.40 (C), 126.45 (2 CH), 126.10 (CH), 125.83 (CH), 53.84 (2 CH_3), 34.99 (CH_2). LC/MS: 357 (M + H). Anal. Calcd for $C_{19}H_{16}N_2O_4S$: C, 60.66; H, 4.53; N, 7.86; S, 9.00. Found C, 60.62; H, 4.58; N, 7.87; S, 9.05.

4.1.5.3. *6-[(2,3-dimethoxyquinoxalin-6-yl)methylthio]nicotinic acid (**9**).* Yield 88%. M.p. 205-206 °C. ν_{max} cm^{-1}: 1710; 1590. λ_{max} nm: 330; 315; 302; 249; 212. ^{1}H-NMR (DMSO-d_6) δ: 8.93 (1H, s, H-6'), 8.05 (1H, d, J=7.2 Hz, H-4'), 7.76 (1H, s, H-5), 7.66 (1H, d, J=7.6 Hz, H-7), 7.56 (1H, d,

J=6.8 Hz, H-3'), 7.44 (1H, d, J=7.6 Hz, H-8), 4.64 (2H, s, CH_2), 4.00 (6H, s, 2 CH_3). ^{13}C-NMR (DMSO-d_6) δ: 166.05 (C), 163.24 (C), 150.19 (CH), 149.93 (C), 149.73 (C), 136.93 (CH), 136.32 (C), 136.29 (C), 135.61 (C), 127.68 (CH), 126.09 (CH), 125.89 (CH), 122.72 (C), 115.08 (CH), 53.87 (2 CH_3), 32.98 (CH_2). LC/MS: 358 (M + H). Anal. Calcd for $C_{17}H_{15}N_3O_4S$: C, 57.13; H, 4.23; N, 11.76; S, 8.97. Found C, 57.09; H, 4.25; N, 11.82; S, 9.01.

4.1.6. General procedure for the preparation of diethyl *N*-{2-[(2,3-dimethoxyquinoxalin-6-yl)methylthio]benzoyl}-L-glutamate (4) and of diethyl *N*-{6-[(2,3-dimethoxyquinoxalin-6-yl)methylthio]nicotinoyl}-L-glutamate (10)

A mixture of the suitable acid **3,9** (1.40 mmol), L-glutamic acid diethyl ester hydrochloride (1.54 mmol), DEPC (1.54 mmol) and TEA (3.08 mmol) in 20 ml of dry DMF was stirred at room temperature, under N_2, for 2 h. The obtained solution was poured in a 40 ml of a 3:1 mixture of ethyl acetate-toluene. This organic phase was washed with water (50 ml), then with a saturated solution of Na_2CO_3 (60 ml), with water again (50 ml) and finally with a saturated solution of NaCl (60 ml). After drying over Na_2SO_4, the solvent was removed by evaporation in vacuo to give compounds **4**, **10** as yellow oils witch were purified by trituration with methanol.

4.1.6.1. *Diethyl N-{2-[(2,3-dimethoxyquinoxalin-6-yl)methylthio]benzoyl}-L-glutamate (**4**).* Yield 38%. M.p. 130-131 °C. ν_{max} cm^{-1}: 3230; 1730; 1700; 1640; 1590; 1225. λ_{max} nm: 315; 301; 233; 197. ^{1}H-NMR (DMSO-d_6) δ: 8.72 (2H, d, NH), 7.72 (1H, s, H-5), 7.65 (1H, d, J=8.0 Hz, H-6'), 7.55 (1H, d, J = 7.6 Hz, H-8), 7.48-7.43 (2H, m, H-7 + H-4'), 7.39 (1H, d, J=7.2 Hz, H-3'), 7.25 (1H, d, , J=7.2 Hz, H-5'), 4.46-7.43 (1H, m, CH), 4.35 (2H, s, CH_2S), 4.12 (2H, q, OCH_2CH_3), 2.28-2.01 (2H, m, CH_2), 1.99-1.79 (2H, m, CH_2), 1.22-1.13 (6H, m, 2 CH_3). ^{13}C-NMR (DMSO-d_6) δ: 172.14 (C), 171.46 (C), 167.82 (C), 149.86 (C), 149.67 (C), 136.30 (C), 135.98 (C),135.54 (C), 135.42 (C), 130.12 (CH), 128.12 (CH), 127.91 (CH), 127.70 (CH), 125.94 (CH), 125.10 (CH), 60.58 (CH_2), 59.86 (CH_2), 53.83 (2 CH_3), 51.63 (CH), 36.33 (CH_2), 29.99 (CH_2), 25.76 (CH_2),

13.99 (2 CH_3). LC/MS: 542 (M + H). Anal. Calcd for $C_{27}H_{31}N_3O_7S$: C, 59.88; H, 5.77; N, 7.76; S, 5.92 Found C, 59.93; H, 5.75; N, 7.82; S, 5.89.

4.1.6.2. *Diethyl N-{6-[(2,3-dimethoxyquinoxalin-6-yl)methylthio]nicotinoyl}-L-glutamate (**10**).* Yield 39%. M.p. 110-111 °C. ν_{max} cm^{-1}: 3330; 1730; 1600; 1630; 1220; 1090; 1020; 990. λ_{max} nm: 330; 315; 303; 273; 248;212.). ^{1}H-NMR ($CDCl_3$) δ: 8.86 (1H, s, H-6'), 7.86 (1H, d, J=8 Hz, Hz H-4'), 7.74 (1H, s, H-5), 7.62 (1H, d, J=8.4 Hz, H-7), 7.46 (1H, d, J=8 Hz, H-3'), 7.16 (1H, d, J=8.4 Hz, H-8), 4.70-4.57 (1H, m, CH), 4.57 (2H, s, CH_2S), 4.15 (2H, q, CH_2CH_3), 4.05 (8H, s, 2 CH_3O + OCH_2CH_3), 2.47-2.37 (2H, m, CH_2CH_2), 2.13-2.04 (2H, m, CH_2CH_2), 1.23 (3H, t, CH_3CH_2). 1.16 (3H, t, CH_3CH_2). ^{13}C-NMR ($CDCl_3$) δ: 173.50 (C), 172.71 (C), 164.89 (C), 162.60 (C), 150.17 (C), 150.00 (C), 147.58 (CH), 137.11 (C), 136.48 (C), 135.99 (C), 135.33 (CH), 127.59 (CH), 126.60 (CH), 126.44 (CH), 125.41 (C), 121.69 (CH), 61.85 (CH_2), 61.01 (CH_2), 54.24 (CH), 52.57 (2 CH_3), 34.38 (CH_2), 30.51 (CH_2), 26.86 (CH_2), 14.16 (2 CH_3). LC/MS: 543 (M + H). Anal. Calcd for $C_{26}H_{30}N_4O_7S$: C, 57.55; H, 5.57; N, 10.33; S, 5.91. Found C, 57.59; H, 5.54; N, 10.29; S, 5.92.

4.1.7. General procedure for the preparation of the *N*-{2-[(2,3-dimethoxyquinoxalin-6-yl)methylthio]benzoyl}-L-glutamic acid (5) and of *N*-{6-[(2,3-dimethoxyquinoxalin-6-yl)methylthio]nicotinoyl]-L-glutamic acid (11)

A mixture of 0.7 mmol of suitable diesther **4**, **10** in 15 ml of ethanol and 8 ml of NaOH 1 N was stirred at room temperature for 3 h. After concentration in vacuo the remaining alkaline solution was diluted with water and made acidic with HCl 2N. Compounds **5**, **11** precipitated from solution and were purified by crystallization from acetonitrile.

4.1.7.1. *N-{2-[(2,3-dimethoxyquinoxalin-6-yl)methylthio]benzoyl}-L-glutamic acid (**5**).* Yield 77%. M.p. 152-153 °C. ν_{max} cm^{-1}: 3250; 1730; 1700; 1640; 1225; 1100; 1035; 990. λ_{max} nm: 331; 317; 249; 212. ^{1}H-NMR ($CDCl_3$) δ: 8.46 (1H, d, J=7.8 Hz, NH), 7.70 (1H, s, H-5), 7.66 (1H, d, J=8.4 Hz, H-8), 7.52-7.49 (2H, m, arom), 7.42-7.15 (3H, m, arom), 4.57-4.48 (1H, m, CH), 4,30 (2H, s, CH_2), 4.07 (6H, s, 2,3-OCH_3), 2.50-1.90 (4H, m, CH_2CH_2). ^{13}C-NMR ($CDCl_3$) δ: 177.90 (C),

175.06 (C), 168.70 (C), 165.44 (C), 150.27 (C), 148.78 (C), 135.96 (C), 134.20 (C), 133.45 (C), 129.46 (CH), 129.07 (CH), 127.68 (CH), 127.56 (CH), 54.89 (2 CH_3), 52.45 (CH), 33.01 (CH_2), 30.96 (CH_2), 26.19 (CH_2). LC/MS: 486 (M + H). Analysis for $C_{23}H_{23}N_3O_7S$: C, 56.90; H, 4.78; N, 8.66; S, 6.60. Found C, 56.94; H, 4.83; N, 8.71; S, 6.66.

4.1.7.2. *N-{6-[(2,3-dimethoxyquinoxalin-6-yl)methylthio]nicotinoyl]-L-glutamic acid (**11**).* Yield 83%. M.p. 101-102 °C. ν_{max} cm^{-1}: 3300; 1735; 1700; 1640; 1590. λ_{max} nm: 329; 315; 302; 271; 248; 212. ^{1}H-NMR ($CDCl_3$) δ: 8.93 (1H, s, H-2'), 8.72 (1H, d, J=7.6 Hz, Hz H-8), 8.07 (1H, d, J=8.4 Hz, H-4'), 7.77 (1H, s, H-5), 7.67 (1H, d, J=6.4 Hz, H-3'), 7.44 (1H, d, J=8.4 Hz, H-7), 4.64 (2H, s, CH_2S), 4.45-4.37 (1H,m, CH), 4.01 (6H, s, 2 CH_3), 2.11-2.07 (2H, m, CH_2), 2.06-1.91 (2H, m, CH_2). ^{13}C-NMR ($CDCl_3$) δ: 173.60 (C), 173.06 (C), 164.62 (C), 161.29 (C), 155.01 (C), 150.15 (C), 148.54 (CH), 136.81 (C), 136.20 (C), 135.59 (CH), 132.15 (C), 127.66 (CH), 126.07 (CH), 125.68 (CH), 125.56 (C), 54.11 (2 CH_3), 52.45 (CH), 32.90 (CH_2), 30.56 (CH_2), 26.12 (CH_2). LC/MS: 487 (M + H). Analysis for $C_{22}H_{22}N_4O_7S$: C, 54.32; H, 4.56; N, 11.52; S, 6.59. Found C, 54.28; H, 4.58; N, 11.49; S, 6.63.

4.2. Cells and viruses

Cell lines were purchased from American Type Culture Collection (ATCC). Cell lines supporting the multiplication of RNA and DNA viruses were the following: CD4+ human T-cells containing an integrated HTLV-1 genome (MT-4); Madin Darby Bovine Kidney (MDBK) [ATCC CCL 22 (NBL-1) *Bos taurus*]; Baby Hamster Kidney (BHK-21) [ATCC CCL 10 (C-13) *Mesocricetus auratus*] and Monkey kidney (Vero-76) [ATCC CRL 1587 *Cercopithecus aethiops*]. Human Immunodeficiency Virus type-1 (HIV-1) IIIB laboratory strain was obtained from the supernatant of the persistently infected H9/IIIB cells (NIH 1983). Viruses representative of ssRNA+ were: i) *Flaviviridae*: yellow fever virus (YFV) [strain 17-D vaccine (Stamaril Pasteur J07B01)], bovine viral diarrhoea virus (BVDV) [strain NADL (ATCC VR-534)]; ii) *Picornaviridae*: enterovirus B [coxsackievirus B5 (CV-B5), strain Ohio-1 (ATCC VR-29)], and enterovirus C [poliovirus type-1

(Sb-1), Sabin strain Chat (ATCC VR-1562)]. Viruses representative of ssRNA- were: iii) *Paramyxoviridae*: human respiratory syncytial virus (RSV) [strain A2 (ATCC VR-1540)]; iv) *Rhabdoviridae*: vesicular stomatitis virus (VSV) [lab strain Indiana (ATCC VR 1540)]. The virus representative of dsRNA was: iv) Reoviridae: reovirus type-1 (Reo-1) [simian virus 12, strain 3651 (ATCC VR-214)]. DNA virus representatives were: v) *Poxviridae*: vaccinia virus (VV) [vaccine strain Elstree-Lister (ATCC VR-1549)]; vi) *Herpesviridae*: human herpes 1 (HSV-1) [strain KOS (ATCC VR-1493)].

4.3. Cytotoxicity assays

Exponentially growing MT-4 cells were seeded at an initial density of 4×10^5 cells/ml in 96-well plates in RPMI-1640 medium, supplemented with 10% fetal bovine serum (FBS), 100 units/ml penicillin G and 100 μg/ml streptomycin. MDBK and BHK cells were seeded in 96-well plates at an initial density of 6×10^5 and 1×10^6 cells/ml, respectively, in Minimum Essential Medium with Earle's salts (MEM-E), L-glutamine, 1 mM sodium pyruvate and 25 mg/l kanamycin, supplemented with 10% horse serum (MDBK) or 10% foetal bovine serum (FBS) (BHK). Vero-76 cells were seeded in 96-well plates at an initial density of 4×10^5 cells/ml, in Dulbecco's Modified Eagle Medium (D-MEM) with L-glutamine and 25 mg/l kanamycin, supplemented with 10% FBS. Cell cultures were then incubated at 37 °C in a humidified, 5% CO_2 atmosphere, in the absence or presence of serial dilutions of test compounds. Cell viability was determined after 48-96 hrs at 37 °C by MTT method for MT-4, MDBK, Vero-76 and BHK [40].

4.4. Antiviral assays

Compound's activity against HIV-1 was based on inhibition of virus-induced cytopathogenicity in exponentially growing MT-4 cell acutely infected with a multiplicity of infection (m.o.i.) of 0.01. Compound's activity against YFV and Reo-1 was based on inhibition of virus-induced cytopathogenicity in BHK-21 cells acutely infected with a m.o.i. of 0.01. Compound's activity against BVDV was based on inhibition of virus-induced cytopathogenicity in MDBK cells acutely infected with a m.o.i. of 0.01. After a 3 or 4-day incubation at 37° C, cell viability was determined

by the MTT method, as described earlier [41]. Compound's activity against CV-B5, Sb-1, VSV, VV, HSV-1 and RSV was determined by plaque reduction assays in infected Vero-76 cell monolayers, as described earlier [41] and the cytotoxicity of test compounds was determined in parallel on the same 96-well plate. Concentrations resulting in 50% or 90% inhibition (CC_{50} or EC_{50}/EC_{90}) were determined by linear regression analysis.

4.5. Yield reduction assay

Vero-76 cells were inoculated with CV-B5 at a m.o.i. of 0.1 in maintenance medium and tested compounds at not cytotoxic concentrations. Following 2 hours adsorption period at 37 °C and 5% CO_2, the inoculum was removed and replaced with fresh medium containing the same concentration of compounds **6**. After 72 hours at 37 °C and 5% CO_2 each sample was harvested and diluted with serial passages, starting from 10^{-1} up to 10^{-8}. The titre of the serial dilutions of the virus-containing supernatant was determined by standard plaque assay, counting the number of obtained plaques in at least two different dilutions for each concentration. Pleconaril was used as reference compound.

4.6. Virucidal activity assay

A CV-B5 suspension containing 5×10^5 PFU/ml was incubated with or without different concentrations of compound for 1 hour at 37 °C. At the end of incubation, the residual infectivity was determined by plaque assay in Vero-76 cells.

4.7. Time-of-drug-addition experiment

Vero-76 cells were infected with CV-B5 at m.o.i. of 0.3. **6** (1 µM) was added at 2 h prior to infection, during the infection and at varying times post infection. The confluent monolayers of Vero-76 cells, seeded in 24-well tissue culture plates, were infected and incubated for 3 days as previously described. Monolayers were collected and the viral titre was determined by plaque assay. Medium containing **6** was: i) added at -2 to 0 (pretreatment) and then removed; ii) added at the time of infection (time 0) and removed or maintained; iii) added at 2, 4, 6, 8 and 12 hours post infection. Pleconaril was used as reference compound.

4.8. Adsorption assays

Vero-76 cells grown in 24-well plate were infected with CV-B5, with a m.o.i. of 0.1, in the presence or absence of compound **6**. Multiwell were incubated for 60 min at 4 °C. Medium containing unadsorbed virus was then removed, cells were washed twice with PBS and covered with MEM containing 1% methylcellulose. Plaques were counted after 24 hrs of incubation at 37 °C.

4.9. Molecular modeling

Compound **6** was parameterized according to a consolidated procedure [17]. The available 3D model structure of the CV-B5 protomer was downloaded from RSCB Protein Data Bank database (pdb code = 1OOP) and optimized via energy relaxation/MD simulations in solution [42-44].

To study the mechanism of VP1 binding, compound **6** was docked into the VP1binding pocket within the protomer complex, and the Molecular Mechanics/Poisson Boltznam Surface-Area (MM/PBSA) [45-47] scoring was adopted to estimate its affinity against the viral target.

In detail, the resulting protein/inhibitor docked conformations were clustered and visualized; then, in the absence of any relevant crystallographic information for the specific compound, the structure of the complex characterized by the lowest interaction energy in the prevailing cluster was selected for further modeling. The selected VP1/**6** complex was then solvated in a TIP3P [48] water box and, then, the required amount of Na^+ and Cl^- ions were added to neutralize the system and to mimic physiological salt conditions (150 mM), removing eventual overlapping water molecules. The solvated systems were subjected to a combination of steepest descent/conjugate gradient minimization of the potential energy, during which all bad contacts were relieved. The relaxed system was then gradually heated to 37 °C in three intervals by running constant volume-constant temperature (NVT) MD simulation. Subsequently, 10 ns MD simulations under isobaric-isothermal (NPT) conditions were conducted to fully equilibrate each solvated compound. The *SHAKE* algorithm with a geometric tolerance of 5×10^{-4} Å was imposed on all covalent bonds involving hydrogen atoms. Temperature control was achieved using the Langevin temperature equilibration scheme and an integration time step of 2 fs. The particle mesh Ewald (PME) method [49] was used

to treat the long-range electrostatics. At this point, this MD runs was followed by other 50 ns of NVT MD simulation. All simulations were carried out using the *Pmemd* modules of Amber 14 [50], running on a hybrid CPU/GPU calculation cluster.

The binding free energy, ΔG_{bind}, between the inhibitor and the VP1 protein was then estimated by resorting to the MM/PBSA approach implemented in Amber 14. According to this well validated methodology, the free energy was calculated for each molecular species (complex, receptor, and ligand), and the binding free energy was computed as the difference:

$$\Delta G_{bind} = G_{VP1/6} - (G_{VP1} + G_6) = \Delta E_{MM} + \Delta G_{SOL} - T\Delta S$$

in which ΔE_{MM} represents the molecular mechanics energy (contributed by van der Waals and electrostatic interactions), ΔG_{SOL} includes the solvation free energy and $T\Delta S$ is the conformational entropy upon ligand binding. The per residue binding free energy decomposition ($\Delta H_{bind,res}$) was performed exploiting the MD trajectory of protein/compound complex, with the aim of identifying the key residues involved in the ligand/protein interaction. This analysis was carried out using the MM/GBSA approach [51, 52], and was based on the same snapshots used in the binding free energy calculation.

Acknowledgments

Authors acknowledge the generous financial support from the “Assessorato della Programmazione, Bilancio, Credito e Assetto del territorio, della Regione Autonoma della Sardegna” (Italy), Grant: Legge Regionale 7 agosto 2007.

References

[1] A.M.Q. King, F. Brown, P. Christian, Picornaviridae, in: M.H.V. Van Regenmortel, C.M. Fauquet, D.H.L. Bishop (Eds.) Virus Taxonomy: The Seventh report of the International Committee on Taxonomy of Viruses. , Academic Press, New York, NY, 2000, pp. 657-673.

[2] J.F. Woodruff, Viral myocarditis. A review, Am. J. Pathol., 101 (1980) 425-484.

[3] R. Kandolf, M. Sauter, C. Aepinus, J.J. Schnorr, H.C. Selinka, K. Klingel, Mechanisms and consequences of enterovirus persistence in cardiac myocytes and cells of the immune system, Virus Res., 62 (1999) 149-158.

[4] H.A. Rotbart, Enteroviral infections of the central nervous system. Clin. Infec. Dis., 20 (1995) 971-981.

[5] J.L. Melnick, Enteroviruses: Polioviruses, coxsackieviruses, echoviruses and newer enteroviruses, in: B.N. Fields, D.M. Knipe, J.L. Melnick, R.M. Chanock, B. Roizmann, R.E. Shope (Eds.) Fields virology, New York, 1985, pp. 739-794.

[6] J.F. Modlin, Coxsackiviruses, echoviruses and newer enteroviruses, in: G.L. Mandel, J.E. Bennett, R. Dolin (Eds.) Principles and practice of infectious diseases, Churchill Livingstone, New York, 1995, pp. 1620-1636.

[7] C.J. Woodall, M.H. Riding, D.I. Graham, G.B. Clements, Sequences specific for enterovirus detected in spinal cord from patients with motor neurone disease, BMJ, 308 (1994) 1541-1543.

[8] J.W. Yoon, The role of viruses and environmental factors in the induction of diabetes, Curr. Top. Microbiol., 164 (1990) 95-123.

[9] B.K. Lim, E.S. Ju, D.H. Lao, S.H. Yun, Y.J. Lee, D.K. Kim, E.S. Jeon, Development of a enterovirus diagnostic assay system for diagnosis of viral myocarditis in humans, Microbiol. Immunol., 57 (2013) 281-287.

[10] L. Andreoletti, T. Bourlet, D. Moukassa, L. Rey, D. Hot, Y. Li, V. Lambert, B. Gosselin, J.F. Mosnier, C. Stankowiak, P. Wattre, Enteroviruses can persist with or without active viral replication in cardiac tissue of patients with end-stage ischemic or dilated cardiomyopathy, J. Infect. Dis., 182 (2000) 1222-1227.

[11] Y. Li, T. Peng, Y. Yang, C. Niu, L.C. Archard, H. Zhang, High prevalence of enteroviral genomic sequences in myocardium from cases of endemic cardiomyopathy (Keshan disease) in China, Heart, 83 (2000) 696-701.

556 [12] A. Muehlenbachs, J. Bhatnagar, S.R. Zaki, Tissue tropism, pathology and pathogenesis of
557 enterovirus infection, J. Pathol., 235 (2015) 217-228.
558 [13] L. Marosova, M. Sojka, J. Precechtelova, D. Stipalova, M. Badurova, M. Borsanyiova, S.
559 Bopegamage, Coxsackievirus infections in pregnant women with a parallel experimental model
560 infection showing possible effects on coarse of pregnancy, Biopolym. Cell. , 27 (2011) 158-161.
561 [14] Q. Zhong, Z. Yang, Y. Liu, H. Deng, H. Xiao, L. Shi, J. He, Antiviral activity of Arbidol
562 against Coxsackie virus B5 in vitro and in vivo, Arch. Virol., 154 (2009) 601-607.
563 [15] I. Briguglio, S. Piras, P. Corona, E. Gavini, M. Nieddu, G. Boatto, A. Carta, Benzotriazole: An
564 overview on its versatile biological behavior, Eur. J. Med. Chem., 97 (2015) 612-648.
565 [16] A. Patidar, J.M.A. Mobiya, G. Selvam, Exploring Potential of Quinoxaline Moiety, Int. J.
566 Pharm. Tech. Res., 3 (2011) 386-392.
567 [17] I. Briguglio, R. Loddo, E. Laurini, M. Fermeglia, S. Piras, P. Corona, P. Giunchedi, E. Gavini,
568 G. Sanna, G. Giliberti, C. Ibba, P. Farci, P. La Colla, S. Pricl, A. Carta, Synthesis, cytotoxicity and
569 antiviral evaluation of new series of imidazo[4,5-g]quinoline and pyrido[2,3-g]quinoxalinone
570 derivatives, Eur. J. Med. Chem., 105 (2015) 63-79.
571 [18] H. Ishikawa, T. Sugiyama, A. Yokoyama, Synthesis of 2,3-bis(halomethyl)quinoxaline
572 derivatives and evaluation of their antibacterial and antifungal activities, Chem. Pharm. Bull., 61
573 (2013) 438-444.
574 [19] A. Carta, G. Paglietti, M.E. Rahbar Nikookar, P. Sanna, L. Sechi, S. Zanetti, Novel substituted
575 quinoxaline 1,4-dioxides with in vitro antimycobacterial and anticandida activity, Chemical, 37
576 (2002) 355-366.
577 [20] A. Carta, M. Palomba, G. Paglietti, P. Molicotti, B. Paglietti, S. Cannas, S. Zanetti,
578 [1,2,3]Triazolo[4,5-h]quinolones. A new class of potent antitubercular agents against multidrug
579 resistant Mycobacterium tuberculosis strains, Bioorg. Med. Chem. Lett., 17 (2007) 4791-4794.
580 [21] J. Neres, R.C. Hartkoorn, L.R. Chiarelli, R. Gadupudi, M.R. Pasca, G. Mori, A. Venturelli, S.
581 Savina, V. Makarov, G.S. Kolly, E. Molteni, C. Binda, N. Dhar, S. Ferrari, P. Brodin, V. Delorme,

582 V. Landry, A.L. de Jesus Lopes Ribeiro, D. Farina, P. Saxena, F. Pojer, A. Carta, R. Luciani, A.
583 Porta, G. Zanoni, E. De Rossi, M.P. Costi, G. Riccardi, S.T. Cole, 2-Carboxyquinoxalines kill
584 Mycobacterium tuberculosis through noncovalent inhibition of DprE1, ACS Chem. Biol., 10 (2015)
585 705-714.
586 [22] A. Carta, M. Loriga, G. Paglietti, A. Mattana, P.L. Fiori, P. Mollicotti, L. Sechi, S. Zanetti,
587 Synthesis, anti-mycobacterial, anti-trichomonas and anti-candida in vitro activities of 2-substituted-
588 6,7-difluoro-3-methylquinoxaline 1,4-dioxides, Eur. J. Med. Chem., 39 (2004) 195-203.
589 [23] N. Kavitha, A. Arun, S.S. Shafi, Synthesis, characterization and antimicrobial activity of some
590 novel s-triazine derivatives incorporating quinoline moiety, Pharma Chemica, 7 (2015) 453-458.
591 [24] A. Carta, M. Loriga, S. Piras, G. Paglietti, P. La Colla, B. Busonera, G. Collu, R. Loddo,
592 Synthesis of variously substituted 3-phenoxymethyl quinoxalin-2-ones and quinoxalines capable to
593 potentiate in vitro the antiproliferative activity of anticancer drugs in multi-drug resistant cell lines,
594 Med. Chem., 2 (2006) 113-122.
595 [25] P. Corona, A. Carta, M. Loriga, G. Vitale, G. Paglietti, Synthesis and in vitro antitumor
596 activity of new quinoxaline derivatives, Eur. J. Med. Chem., 44 (2009) 1579-1591.
597 [26] A.A. Abu-Hashem, M.A. Gouda, F.A. Badria, Synthesis of some new
598 pyrimido[2',1':2,3]thiazolo[4,5-b]quinoxaline derivatives as anti-inflammatory and analgesic agents,
599 Eur. J. Med. Chem., 45 (2010) 1976-1981.
600 [27] A. Carta, S. Piras, G. Paglietti, S. Pricl, P. La Colla, B. Busonera, R. Loddo, 2(3)-Aryl-
601 thio(oxy)-methylquinoxaline derivatives: a new class of P-glycoprotein-mediated drug efflux
602 inhibitors, Med. Chem., 4 (2008) 194-205.
603 [28] Y.N.P. Deepika, K. Sachin, S. Shewta, Biological activity of quinoxaline derivatives, Inter. J.
604 Curr. Pharm. Rev. Res., 1 (2011) 33-46.
605 [29] L. You, E.J. Cho, J. Leavitt, L.C. Ma, G.T. Montelione, E.V. Anslyn, R.M. Krug, A. Ellington,
606 J.D. Robertus, Synthesis and evaluation of quinoxaline derivatives as potential influenza NS1A
607 protein inhibitors, Bioorg. Med. Chem. Lett., 21 (2011) 3007-3011.

608 [30] A. Husain, D. Madhesia, Recent advances in pharmacological activities of
609 quinoxalinederivates, J. Pharm. Res., 4 (2011) 924-929.
610 [31] I.A.I. Ali, I.A. Al-Masoudi, H.G. Hassan, N.A. Al-Masoudi, Synthesis and anti-HIV activity of
611 new homo acyclic nucleosides, 1-(pent-4-enyl)quinoxalin-2-ones and 2-(pent-4-
612 3nyloxy)quinoxalines, Chem. Heterocyc. Compd., 43 (2007).
613 [32] M. Loriga, G. Vitale, G. Paglietti, Quinoxaline chemistry. Part 9. Quinoxaline analogues of
614 trimetrexate (TMQ) and 10-propargyl-5,8-dideazafolic acid (CB 3717) and its precursors. Synthesis
615 and evaluation of in vitro anticancer activity, Farmaco, 53 (1998) 139-149.
616 [33] K.M. Hussain, K.L. Leong, M.M. Ng, J.J. Chu, The essential role of clathrin-mediated
617 endocytosis in the infectious entry of human enterovirus 71, J. Biol. Chem., 286 (2011) 309-321.
618 [34] X.K. Tong, H. Qiu, X. Zhang, L.P. Shi, G.F. Wang, F.H. Ji, H.Y. Ding, W. Tang, K. Ding, J.P.
619 Zuo, WSS45, a sulfated alpha-D-glucan, strongly interferes with Dengue 2 virus infection in vitro,
620 Acta Pharmacol. Sin., 31 (2010) 585-592.
621 [35] P. Jiang, Y. Liu, H.C. Ma, A.V. Paul, E. Wimmer, Picornavirus morphogenesis, Microbiol.
622 Mol. Biol. Rev., 78 (2014) 418-437.
623 [36] M.G. Rossmann, E. Arnold, J.W. Erickson, E.A. Frankenberger, J.P. Griffith, H.J. Hecht, J.E.
624 Johnson, G. Kamer, M. Luo, A.G. Mosser, et al., Structure of a human common cold virus and
625 functional relationship to other picornaviruses, Nature, 317 (1985) 145-153.
626 [37] A.T. Hadfield, G.D. Diana, M.G. Rossmann, Analysis of three structurally related antiviral
627 compounds in complex with human rhinovirus 16, Proc. Natl. Acad. Sci. U.S.A., 96 (1999) 14730-
628 14735.
629 [38] R. Fuchs, D. Blaas, Uncoating of human rhinoviruses, Rev. Med. Virol., 20 (2010) 281-297.
630 [39] M. Loriga, G. Paglietti, Quinoxaline chemistry. Part 1. 6-trifluoromethylquinoxalines and their
631 N-oxides. synthesis and structure elucidation., J. Chem. Res., (1986) 277-296.

632 [40] R. Pauwels, J. Balzarini, M. Baba, R. Snoeck, D. Schols, P. Herdewijn, J. Desmyter, E. De
633 Clercq, Rapid and automated tetrazolium-based colorimetric assay for the detection of anti-HIV
634 compounds, J. Virol. Methods, 20 (1988) 309-321.
635 [41] G. Sanna, P. Farci, B. Busonera, G. Murgia, P. La Colla, G. Giliberti, Antiviral properties from
636 plants of the Mediterranean flora, Nat. Prod. Res., 29 (2015) 2065-2070.
637 [42] L. Brambilla, D. Genini, E. Laurini, J. Merulla, L. Perez, M. Fermeglia, G.M. Carbone, S.
638 Pricl, C.V. Catapano, Hitting the right spot: Mechanism of action of OPB-31121, a novel and potent
639 inhibitor of the Signal Transducer and Activator of Transcription 3 (STAT3), Mol. Oncol., 9 (2015)
640 1194-1206.
641 [43] E. Laurini, D. Marson, V. Dal Col, M. Fermeglia, M.G. Mamolo, D. Zampieri, L. Vio, S. Pricl,
642 Another brick in the wall. Validation of the sigma1 receptor 3D model by computer-assisted design,
643 synthesis, and activity of new sigma1 ligands, Mol. Pharm., 9 (2012) 3107-3126.
644 [44] S. Pricl, B. Cortelazzi, V. Dal Col, D. Marson, E. Laurini, M. Fermeglia, L. Licitra, S. Pilotti,
645 P. Bossi, F. Perrone, Smoothened (SMO) receptor mutations dictate resistance to vismodegib in
646 basal cell carcinoma, Mol. Oncol., 9 (2015) 389-397.
647 [45] S. Brune, D. Schepmann, K.H. Klempnauer, D. Marson, V. Dal Col, E. Laurini, M. Fermeglia,
648 B. Wunsch, S. Pricl, The sigma enigma: in vitro/in silico site-directed mutagenesis studies unveil
649 sigma1 receptor ligand binding, Biochemistry, 53 (2014) 2993-3003.
650 [46] A. Carta, I. Briguglio, S. Piras, G. Boatto, P. La Colla, R. Loddo, M. Tolomeo, S. Grimaudo,
651 A. Di Cristina, R.M. Pipitone, E. Laurini, M.S. Paneni, P. Posocco, M. Fermeglia, S. Pricl, 3-Aryl-
652 2-[1H-benzotriazol-1-yl]acrylonitriles: a novel class of potent tubulin inhibitors, Eur. J. Med.
653 Chem., 46 (2011) 4151-4167.
654 [47] G. Giliberti, C. Ibba, E. Marongiu, R. Loddo, M. Tonelli, V. Boido, E. Laurini, P. Posocco, M.
655 Fermeglia, S. Pricl, Synergistic experimental/computational studies on arylazoenamine derivatives
656 that target the bovine viral diarrhea virus RNA-dependent RNA polymerase, Bioorg. Med. Chem.,
657 18 (2010) 6055-6068.

[48] W.L. Jorgensen, J. Chandrasekhar, J.D. Madura, R.W. Impey, M.L. Klein, Comparison of simple potential functions for simulating liquid water, J. Chem. Phys., 79 (1983) 926-935.

[49] A. Toukmaji, C. Sagui, J. Board, T. Darden, Efficient particle-mesh Ewald based approach to fixed and induced dipolar interactions., J. Chem. Phys., 113 (2000) 10913−10927.

[50] D.A. Case, J.T. Berryman, R.M. Betz, D.S. Cerutti, T.E.I. Cheatham, T.A. Darden, R.E. Duke, T.J. Giese, H. Gohlke, A.W. Goetz, N. Homeyer, S. Izadi, P. Janowski, J. Kaus, A. Kovalenko, T.S. Lee, S. LeGrand, P. Li, T. Luchko, R. Luo, B. Madej, K.M. Merz, G. Monard, P. Needham, H. Nguyen, H.T. Nguyen, I. Omelyan, A. Onufriev, D.R. Roe, A. Roitberg, R. Salomon-Ferrer, C.L. Simmerling, W. Smith, J. Swails, R.C. Walker, J. Wang, R.M. Wolf, X. Wu, AMBER 2015, D.M. York and P.A. Kollman, University of California, San Francisco, 2015.

[51] A. Onufriev, D. Bashford, D.A. Case, Modification of the generalized born model suitable for macromolecules., J. Phys. Chem. B, 104 (2000) 3712-3720.

[52] V. Tsui, D.A. Case, Theory and applications of the generalized Born solvation model in macromolecular simulations, Biopolymers, 56 (2000) 275-291.

Figure legends

Figure 1. Chemical structure of quinoxaline derivatives endowed with antiviral activity.

Figure 2. Chemical structure of quinoxaline derivatives **2a-e, 3-11**.

Figure 3. Dose-dependent reduction of CV-B5 titre in the presence of different concentrations of **6** (dark bars), compared with untreated infected control (striped bars); pleconaril was used as reference compound (light bars). Data represent mean ± S.D. values of two independent determinations.

Figure 4. 6 inhibition of CV-B5 in a time of drug addition experiment. The addition of **6** at 0 and 2 hours significantly reduces the virus titre, while when added 4 hours or more post infection, **6** is not more able to protect the Vero-76 cells (squares). Virus titres were compared with the untreated virus

(triangles) and with a reference compound (circles) in the same experimental conditions. The results are representative of two independent experiments, each one performed in duplicate.

Figure 5. Overall representation of the optimized and solvated CV-B5 protomer with compound **6** docked into the pocket of VP1. The inhibitor is in firebrick sphere representation while the protomer is represented by its different monomer highlighted in colors as follows: VP1, green;, VP2, blue; VP3, dark magenta; and VP4, gold.

Figure 6. (A) Details of compound **6** in the VP1 binding pocket of the CV-B5 protomer complex. Compound **6** is depicted as atom-colored sticks-and-balls (C, gray; N, blue, Cl, green; S, yellow). Hydrogen bonds are highlighted as black broken lines. The side chains of all VP1 residues mainly involved in the interaction with **6** are highlighted as colored sticks: I94, L106, F114, L116, L118, Y191, and M215, magenta; T96 and R103, green; R97 and F239, cyan. Hydrogen atoms, water molecules, ions and counterions are omitted for clarity. (B) Per residue binding enthalpy decomposition DHbind,res for compound **6** in complex with VP1. The corresponding enthalpic contribution for each critical protein residues are colored according to the specific underlying interactions interactions: I94, L106, F114, L116, L118, Y191, and M215, hydrophobic interaction (magenta); T96 and R103, hydrogen bond (green); R97 and F239, p interactions (cyan).

Scheme 1. Synthesis scheme of 2,3-dimethoxy-6-[(arylthio)methyl]quinoxaline derivatives **2a-e**, **3-5**. Reaction condition: *i*) DMF, Cs_2CO_3, 70 °C, 2 h; *ii*) EtOH/H_2O, NaOH 1M, 70 °C, 7 h; *iii*) L-glutamic acid diethyl ester hydrochloride, DMF, DEPC, TEA, r.t., 2 h; *iv*) EtOH, NaOH 1M, r.t., 3 h.

Scheme 2. Synthesis of 2,3-dimethoxy-6-[(phenylthio)methyl]quinoxaline derivatives **6-7** and 2,3-dimethoxy-6-[(pyridin-2-ylthio)methyl]quinoxaline derivatives **8-11**. Reaction condition: *i*) DMF, r.t., 5 days; *ii*) EtOH/H2O, NaOH 1M, 70 °C, 7 h; *iii*) L-glutamic acid diethyl ester hydrochloride, DMF, DEPC, TEA, r.t., 2 h; *iv*) EtOH, NaOH 1M, r.t., 3 h. *v*) DMF, Cs_2CO_3, 70 °C, 2 h; *vi*) EtOH, $NaBH_4$, N_2, r.t., 30 min.

Figure 1

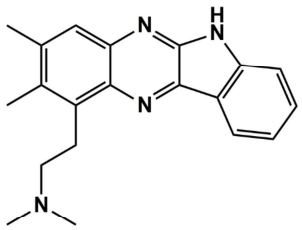

(A)
Anti-HSV-1, cytomegalovirus, and varicella-zoster activity

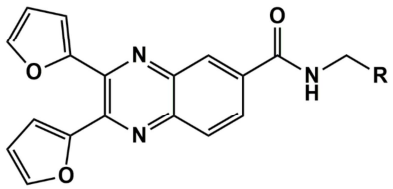

(B)
Anti-Influenza activity

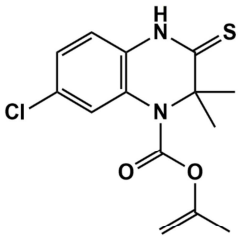

(C)
Anti-HIV1 activity

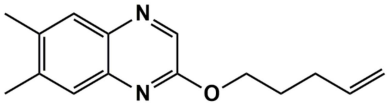

(D)
Anti-HIV1 activity

Figure 3

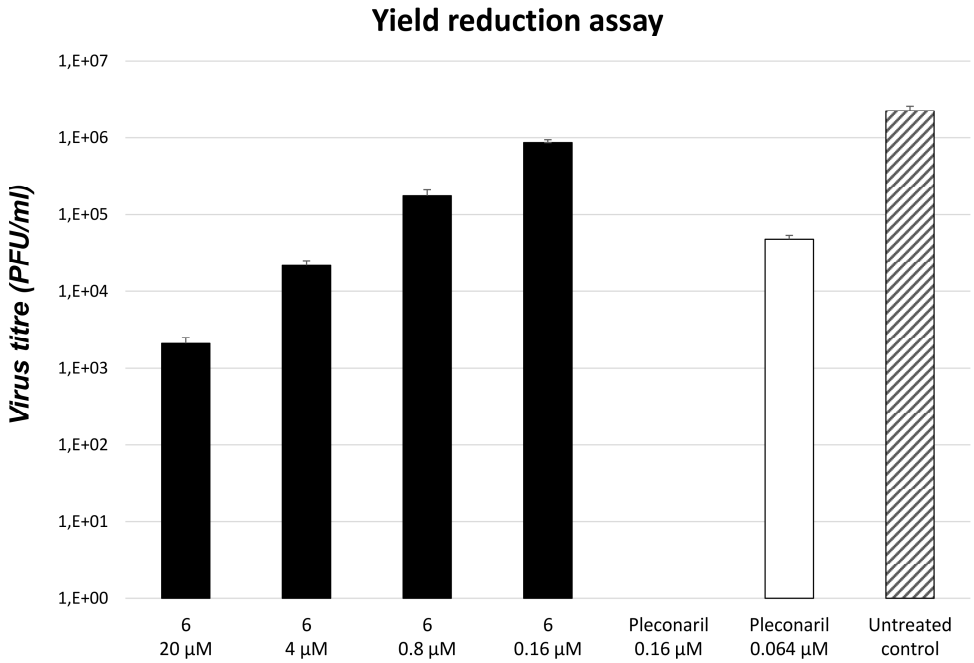

Figure 4

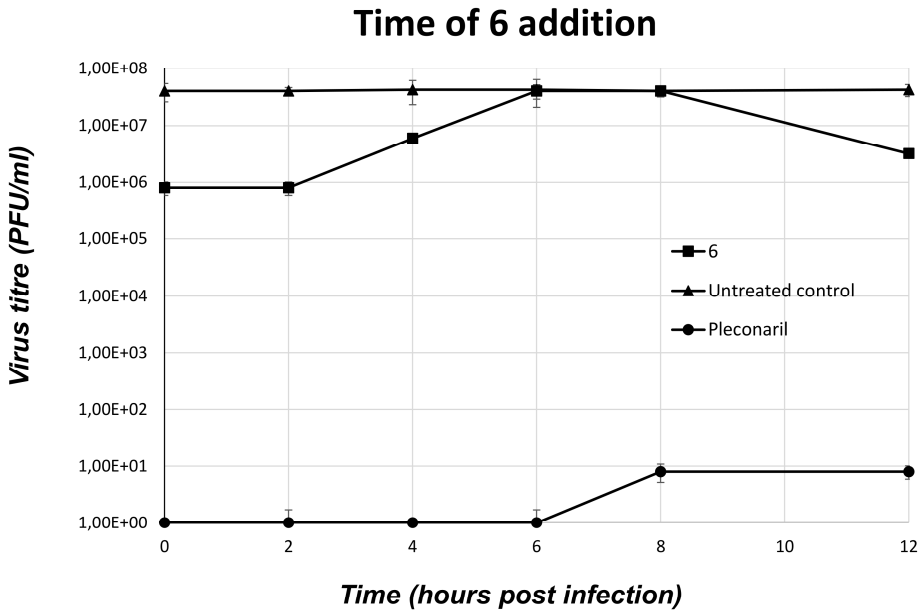

Figure 5

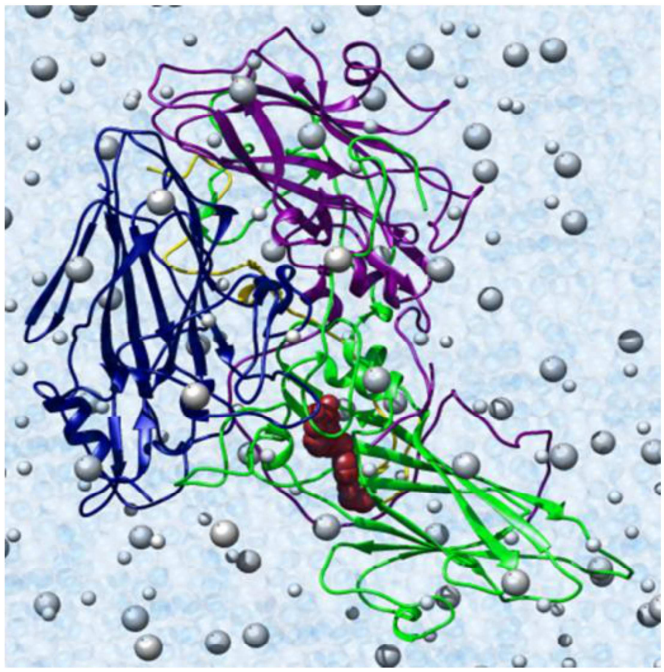

Figure 6

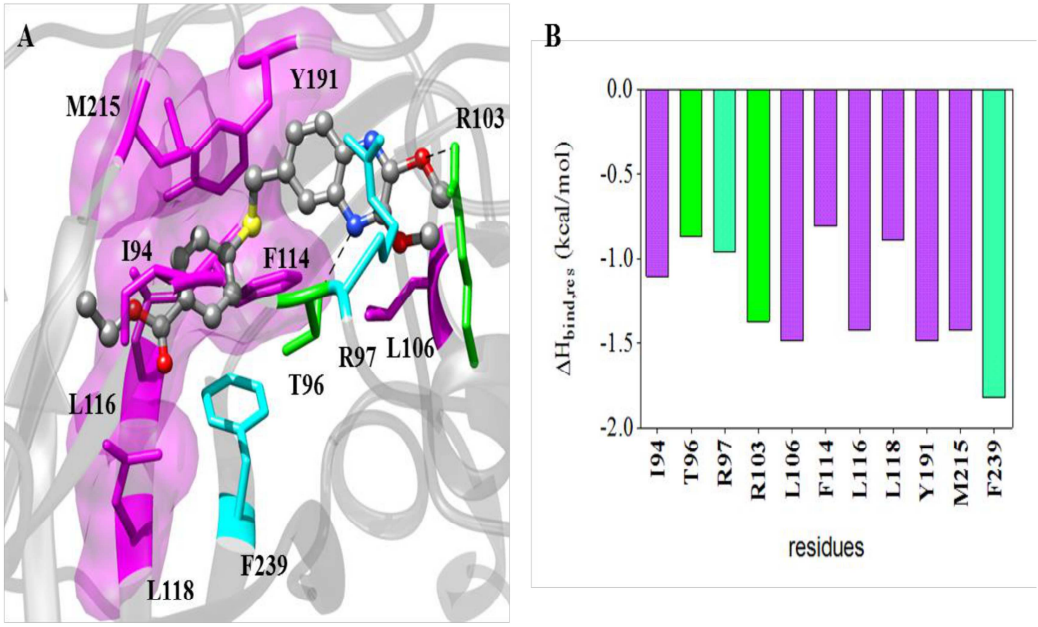

Scheme 2

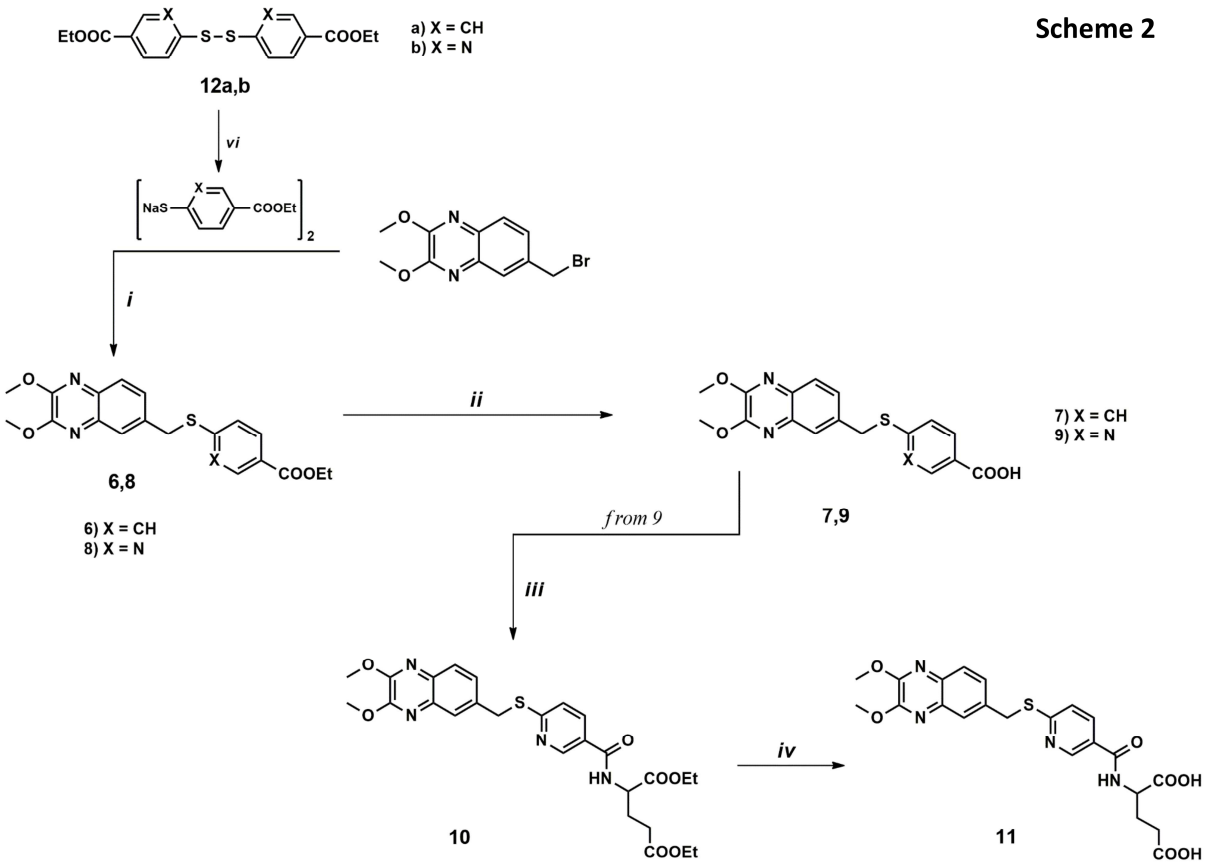

Figure 2

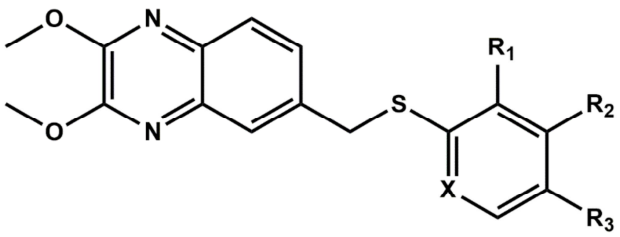

2a-e, 3-11

2a) X = CH, R_1=H, R_2=H, R_3=OCH_3,
2b) X = CH, R_1=H, R_2=Cl, R_3=Cl
2c) X = CH, R_1=H, R_2 -R_3=CH=CH-CH=CH
2d) X = CH, R_1=$COOCH_3$, R_2=H, R_3=H
2e) X = N, R_1 -R_2 -R_3=H
3) X = CH, R_1=COOH, R_2=H, R_3=H
4) X = CH, R_1= CO-Glu-Et, R_2=H, R_3=H
5) X = CH, R_1 = CO-Glu-H, R_2=H, R_3=H
6) X = CH, R_1=H, R_2=H, R_3=COOEt
7) X = CH, R_1=H, R_2=H, R_3=COOH
8) X = N, R_1=H, R_2=H, R_3=COOEt
9) X = N, R_1=H, R_2=H, R_3=COOH
10) X = N, R_1=H, R_2=H, R_3=CO-Glu-Et
11) X = N, R_1=H, R_2=H, R_3= 3-CO-Glu-H

Scheme 1

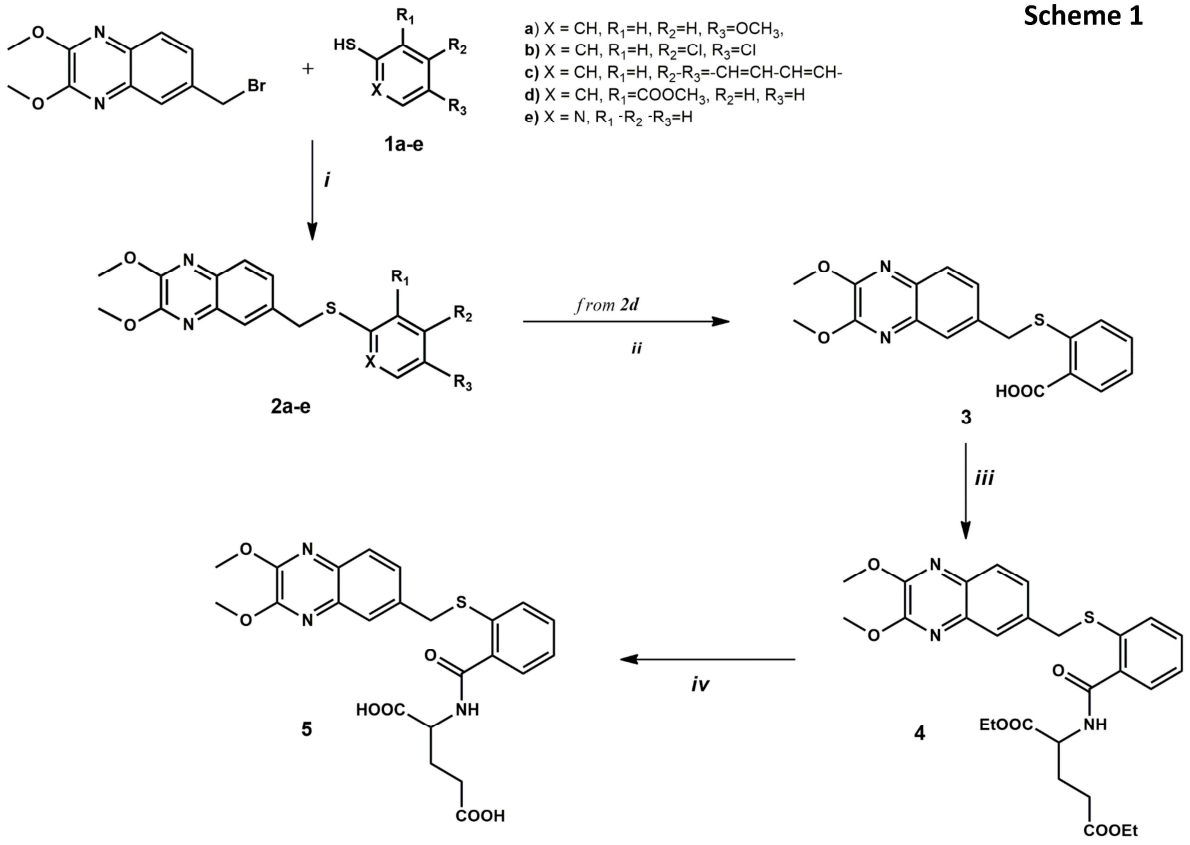

Highlights

New quinoxaline derivatives were tested against different RNA and DNA viruses.

Three compounds emerged for their very potent antiviral activity against CV-B5.

Compound 6 inhibits by targeting the penetration or an early event of life cycle.

Molecular simulations revealed that a possible viral target is the viral capsid protein VP1.